Electron-Impact Dissociation of Methane into CH₃ and CH₂ Radicals
II. Absolute Cross Sections

Tohru NAKANO, Hirotaka TOYODA and Hideo SUGAI

Department of Electrical Engineering, Nagoya University, Furo-cho, Chikusa-ku, Nagoya 464-01

The electron energy dependence of partial cross sections for dissociation of methane into CH_3 and CH_2 radicals has been reported in part I of this paper. In order to assign absolute values to these relative cross sections, two additional experiments were carried out. One was cross-section measurement for electron-impact nitrogen dissociation ($N_2 \rightarrow N+N$, $N+N^+$) using threshold-ionization mass spectrometry. The other was the measurement of sticking coefficients of CH_3, CH_2, and atomic nitrogen. According to these measurements, the absolute partial cross sections for neutral dissociation were determined: maximum cross section is 1.4×10^{-20} m^2 at 24 eV for CH_3 radical and 0.72×10^{-20} m^2 at 18 eV for CH_2 radical.

§1. Introduction

Much attention has been given to the measurement of cross sections for electron impact dissociation of molecules into neutral radicals since these cross sections are parameters essential to the understanding and control of various plasma processes. However, it is extremely difficult to detect neutral fragments, and so far, only the total dissociation cross section for electron methane collisions has been measured by the surface adsorption method.[1] In order to obtain partial cross sections, we have adopted threshold-ionization mass spectrometry, which is a promising tool for detecting neutral radicals with a very high sensitivity.[2-4] In part I of this paper, we reported, for the first time to our knowledge, the electron energy dependence of the partial cross sections for the dissociation of methane into CH_3 and CH_2 radicals. However, these cross sections are still relative ones.

In part II of this paper, we report the calibration procedures and the resultant absolute cross sections. We describe how to calibrate the relative values in §2, and subsequently, the result of two complementary measurements is presented in §3. Finally, the absolute partial cross sections are given in §4, together with discussion and comparison with relevant previous reports.

§2. Calibration Procedure

Figure 1 shows a schematic diagram of the experimental setup to measure cross sections for neutral dissociation, which has been described in part I of this paper. Suppose that a primary electron beam of current I_c collides with methane to yield CH_3 radicals at a production rate G in a dissociation cell (volume V and inner surface area A). These radicals disappear at a loss rate L due to collisions in the gas phase, and they are also lost on the wall surface since mean free paths are larger than geometrical dimensions of the cell. On the other hand, radicals are evacuated through two orifices into a detection cell and an electron source cell with the vacuum conductances C_a and C_b, respectively. The conservation of a particle number density yields the time variation of CH_3 radical density n in the dissociation cell:

$$V\frac{dn}{dt}=G-kn-L-(C_a+C_b)n, \qquad (1)$$

where the first term on the right-hand side (RHS) is given by $G=\sigma l[CH_4]I_c/e$ (see eq.(2) in part I of this paper). The second term on the RHS corresponds to the surface loss expressed by a rate constant $k=svA/4$, where s is the sticking coefficient (probability) and v is the radical speed. The gas-phase loss term L is mainly caused by the recombination process $CH_3+CH_3 \rightarrow C_2H_6$, and the recombination rate constant[4] ($r=8 \times 10^{-11}$ cm^3/s) yields $L \simeq rn^2$, which is much less than the surface loss term (kn). The fourth term on the RHS of eq. (1) denotes the evacuation loss due to differential pumping.

The radical density n_0 in the steady state is obtained with $dn/dt=0$ and $L=0$ in eq. (1), through

$$n_0=G/(k+C_a+C_b). \qquad (2)$$

The CH_3 radical effuses with the flux $C_a n_0$ through the orifice into the detection cell. The radical density [CH_3]
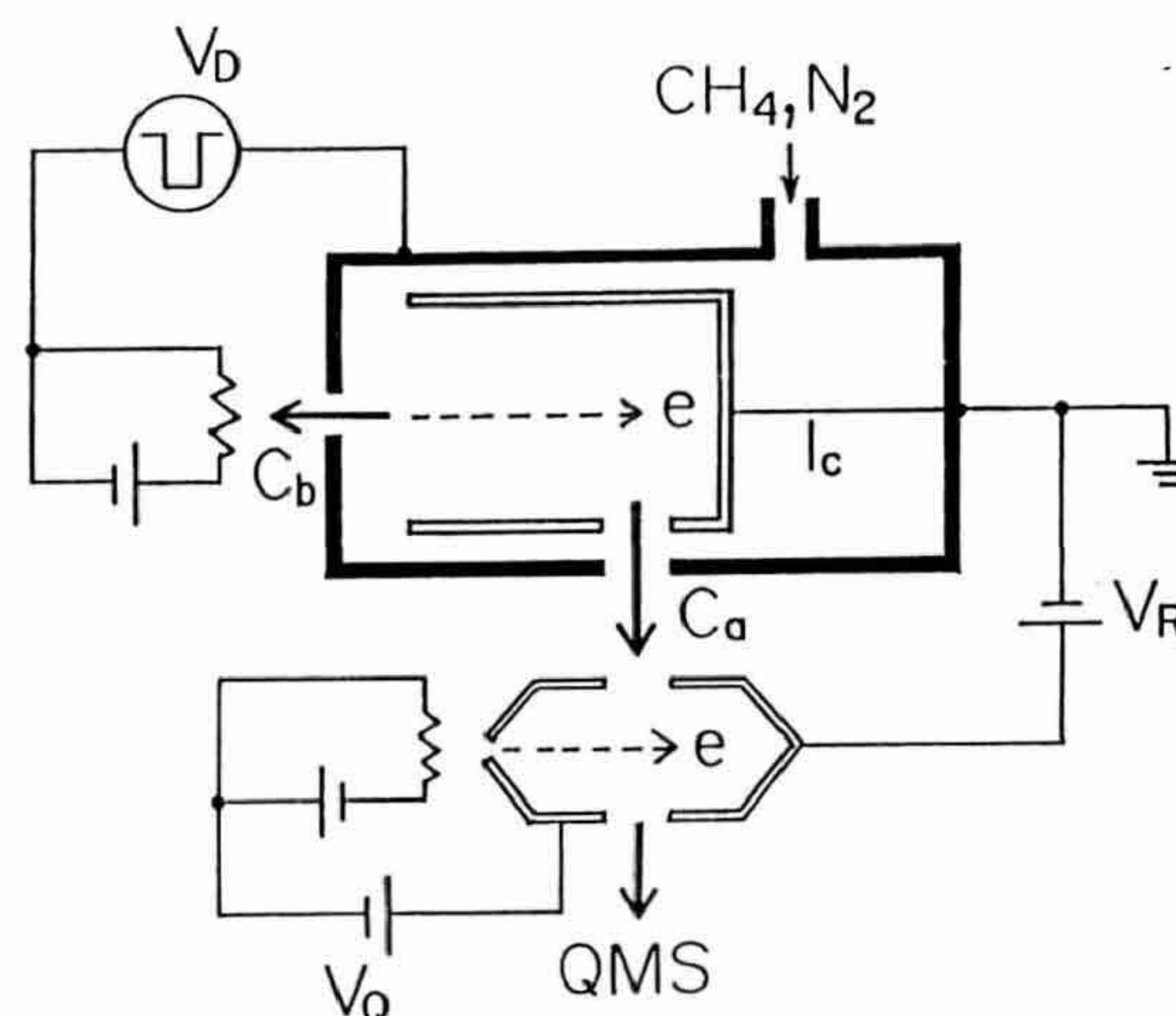

Fig. 1. Schematic diagram of experimental setup.

in the ionization chamber is proportional to this flux, and hence $[CH_3] = \eta C_a n_0$ (η = const.). Thus, the production rate G' of CH_3^+ ions can be expressed, from eq. (3) in part I of this paper, by

$$G' = \sigma' l' \eta C_a n_0 I' / e. \qquad (3)$$

The output signal dS/dt of the quadrupole mass spectrometer (QMS) is proportional to G', so that we can derive the partial dissociation cross section from eqs. (2) and (3) as

$$\sigma = \left(\frac{\eta'}{\beta}\right) \cdot \frac{k + C_a + C_b}{\sigma'[CH_4]C_a} \cdot \frac{dS}{dt}, \qquad (4)$$

where η' is a constant and $\beta = ll' I_c I' / e^2$.

In order to calculate the absolute cross section in eq. (4) from the measured dS/dt, we must know the values of C_a, C_b, k, and the proportional constant η'/β. Firstly, the vacuum conductances of the two orifices are easily found from methane pressure measurements to be $C_a = 1.02$ l/s and $C_b = 0.58$ l/s for CH_4. In general, the vacuum conductance depends on the geometry of the orifice and is inversely proportional to the square root of mass, so that the conductances for CH_3, CH_2 and atomic nitrogen can be calculated from those for CH_4. Secondly, let us estimate the surface loss rate k by measuring the time decay of radical densities after turning the primary electron beam off ($G=0$). We find the solution of eq. (1) with $G=L=0$ to be

$$n(t) = n_0 \exp(-t/\tau), \qquad (5)$$

where the time constant is given by

$$\tau = V/(k + C_a + C_b). \qquad (6)$$

Thus, the measurement of the time constant τ enables the estimation of the value of k and the sticking coefficient s for CH_3 radical. The same procedure can be applied to CH_2 radicals and atomic nitrogen.

Finally, the proportional constant η'/β can be obtained when we compare known cross sections for a certain species with the relative values measured for the same species in our experimental setup. To do this, we have carefully selected nitrogen gas since the mass of the nitrogen atom ($m/e = 14$) is very close to the mass of CH_3 or CH_2 and hence, the mass discrimination effect can be minimized. Electron nitrogen collision gives rise to atomic nitrogen via two processes: neutral dissociation $N_2 \rightarrow N + N$, and dissociative ionization $N_2 \rightarrow N + N^+$. Cosby[5] has recently measured the cross section σ_{dn} for neutral dissociation, and Rapp and Englander-Golden[6] have reported the cross section σ_{di} for dissociative ionization, while Winters[7] has measured the total dissociation cross section ($\sigma_{dn} + \sigma_{di}$). When we count the number of nitrogen atoms by means of threshold-ionization mass spectrometry, the QMS output dS/dt is proportional to ($2\sigma_{dn} + \sigma_{di}$) since an event of neutral dissociation yields two nitrogen atoms. Therefore, on the analogy of eq. (4), we have the cross section for nitrogen atom production as

$$2\sigma_{dn} + \sigma_{di} = \left(\frac{\eta'}{\beta}\right) \cdot \frac{k_N + C_{aN} + C_{bN}}{\sigma'_N [N_2] C_{aN}} \cdot \frac{dS}{dt}, \qquad (7)$$

where the subscript N indicates the quantity of atomic nitrogen and $[N_2]$ denotes the number density of nitrogen molecules. All parameters involved in eq. (7) are known except for η'/β, so that we can determine the proportional constant η'/β.

§3. Complementary Measurements

Two additional measurements in the identical dual-electron-beam device are necessary for the absolute-value calibration described in §2. One is the measurement of nitrogen dissociation to determine the constant η'/β, and the other is the measurement of the surface loss constant k. First of all, the applicability of threshold-ionization mass spectrometry to the detection of atomic nitrogen was checked. Instead of methane, nitrogen gas was introduced into the dissociation cell at a pressure of 10^{-3}–10^{-2} Pa. Before turning the primary beam on, the QMS output for $m/e = 14(N^+)$ was measured as a function of the probing beam energy E_Q, as indicated by closed circles in Fig. 2. The threshold energy for dissociative ionization ($N_2 \rightarrow N + N^+$) turned out to be about 30 eV, in accordance with the previous report.[6] When the primary electron beam is injected into the dissociation cell, electron nitrogen collision gives rise to atomic nitrogen, and a new signal appears at lower energies of the probing beam, as indicated by open circles in Fig. 2. This signal comes from the ionization of atomic nitrogen whose threshold[8] is 14.5 eV. Thus, atomic nitrogen can be detected when 15 eV < E_Q < 25 eV.

Setting the value of E_Q at 20 eV, we measured the production rate of atomic nitrogen as a function of the primary beam energy. The experimental method is the same one that has been used for CH_3 and CH_2 radicals (see part I of this paper). For instance, N_2^+ and N^+ ions in the dissociation cell were prevented from entering the
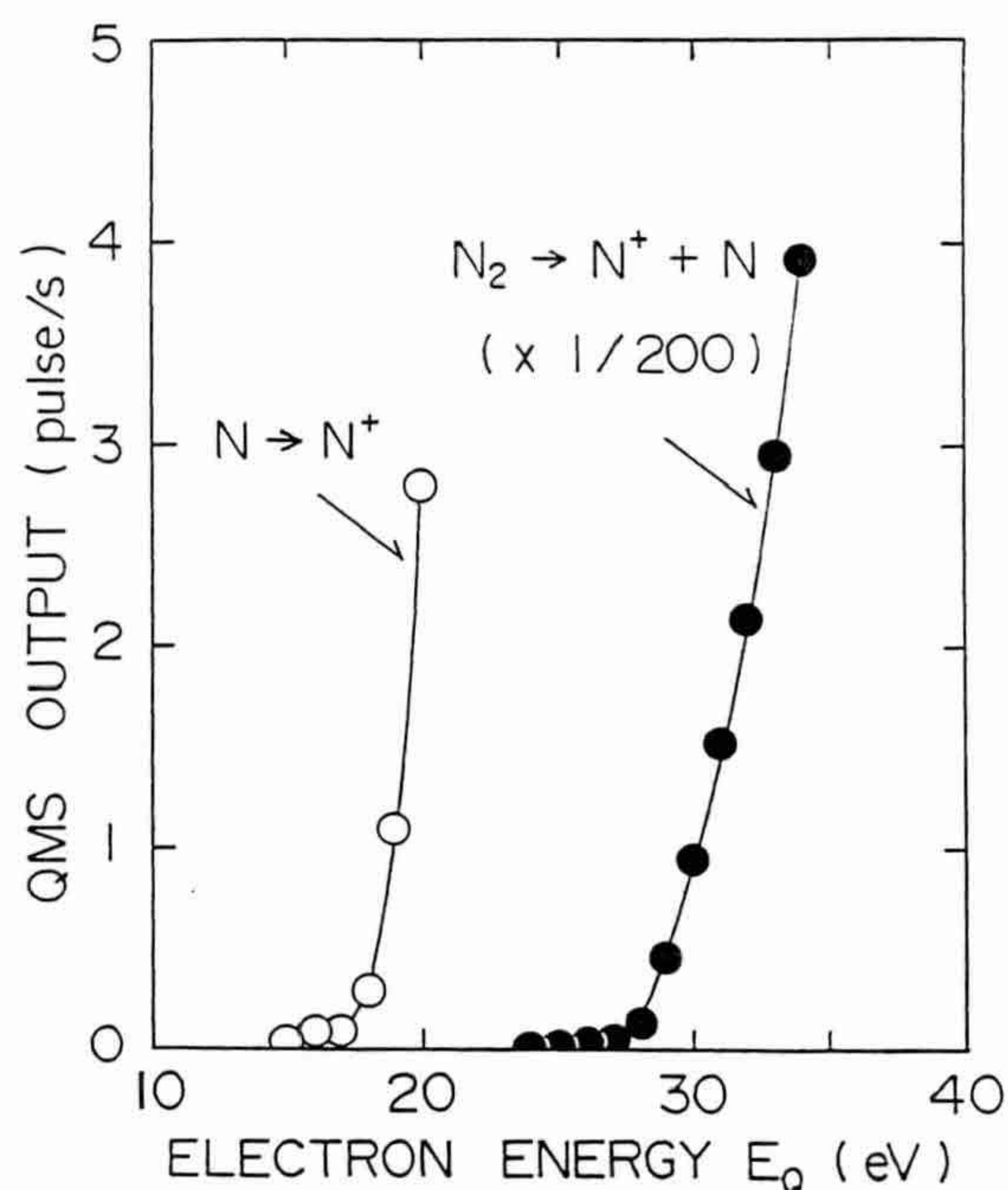

Fig. 2. Quadrupole-mass-spectrometer output for $m/e = 14(N^+)$ as a function of probing beam energy with the primary beam on (open circle) and the beam off (closed circle). $I_c = 1.4$ μA and $V_D = 30$ V. The vertical scale for closed circles is reduced by a factor of 200.
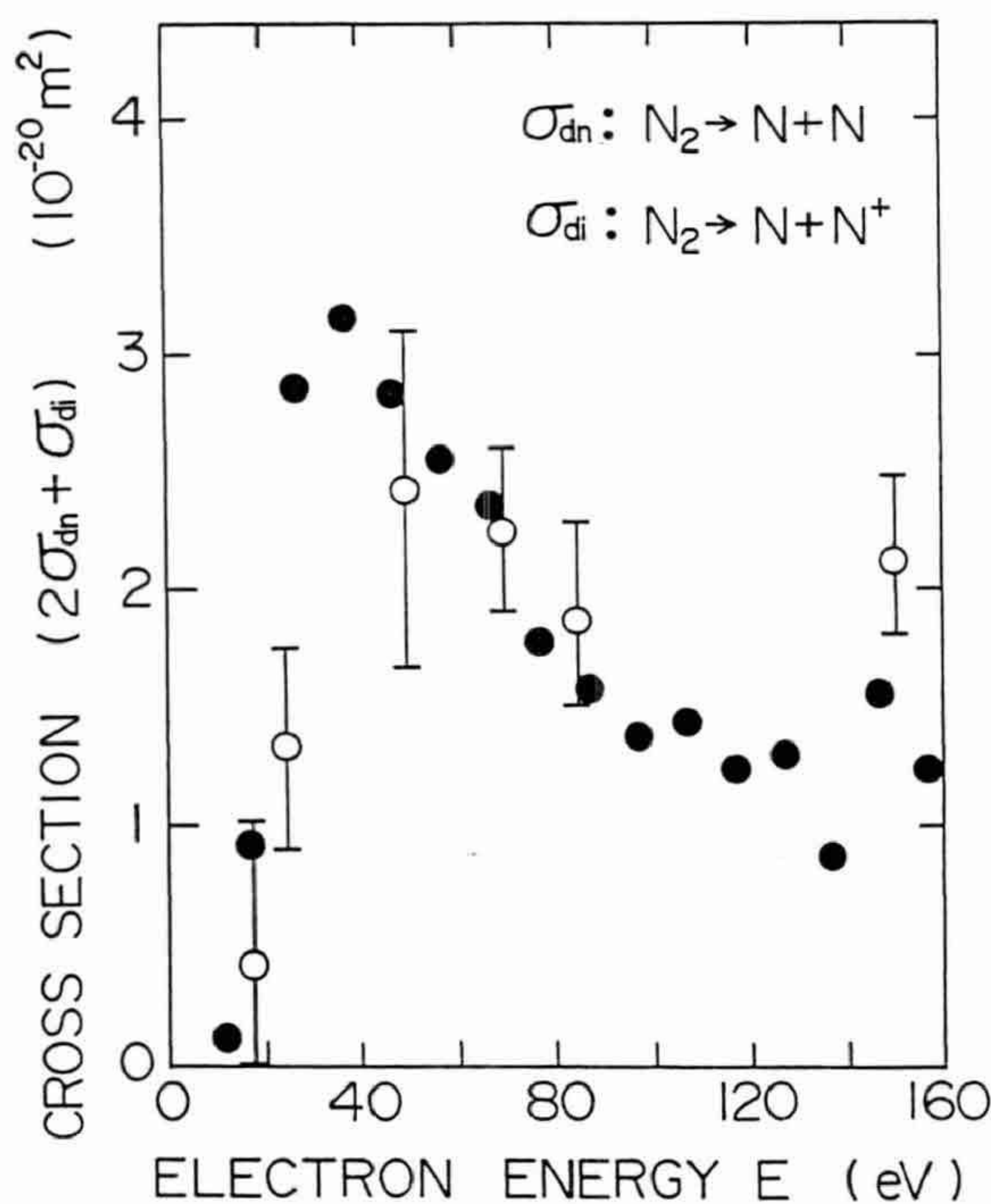
Fig. 3. Cross section ($2\sigma_{dn} + \sigma_{di}$) for production of atomic nitrogen as a function of electron impact energy. Closed circle indicates the present relative values and open circle Cosby's and Rapp and Englander-Golden's absolute values.

Fig. 4. Density decay after turning off of the electron beam for (a) atomic nitrogen and (b) CH_3 and CH_2 radicals.

detection cell by the positive bias V_R shown in Fig. 1. The measured production rate of N atoms, that is, dS/dt in eq. (7), is indicated by closed circles in Fig. 3. The threshold energy for nitrogen dissociation is found to be ~ 10 eV in accordance with the previous report.[7] As stated in §2, the measured output dS/dt is proportional to ($2\sigma_{dn} + \sigma_{di}$). The absolute cross section of ($2\sigma_{dn} + \sigma_{di}$) can be obtained from Cosby's data[5] of σ_{dn} and Rapp and Englander-Golden's data[6] of σ_{di}, as indicated by open circles in Fig. 3. Fitting our relative cross sections to the absolute scale was done as follows. The difference between the present data and Cosby's and Rapp and Englander-Golden's data at six different energies was minimized by a least-squares method. In this manner, the proportional constant η'/β was obtained from eq. (7), where the surface loss rate k_N will be discussed below.

The time behavior of CH_3, CH_2 and N after the primary beam was switched off was investigated to obtain information on the surface loss rate. The electron beam was chopped by a 30-V square-wave voltage $V_D(t)$ at a repetition frequency of 20 Hz. The QMS output signal was accumulated as a function of time over 4×10^5 shots of the pulsed beam. After turning off, the radical signal decreased with time and reached a stationary value at ~ 20 msec, which was caused by impurity gases. We subtracted this stationary value from the raw data, normalized the corrected value with the initial value, and plotted this on a semilogarithmic scale, as shown in Fig. 4. The densities of N, CH_3, and CH_2 decay exponentially with time. The slope of the solid line indicated in Fig. 4 provides the decay time constant τ in eq. (6). Table I shows the measured time constant, the surface loss rate, and the sticking coefficient where the volume $V = 15$ cm^3, the surface area $A = 62$ cm^2, and the radical speed $v = (8$
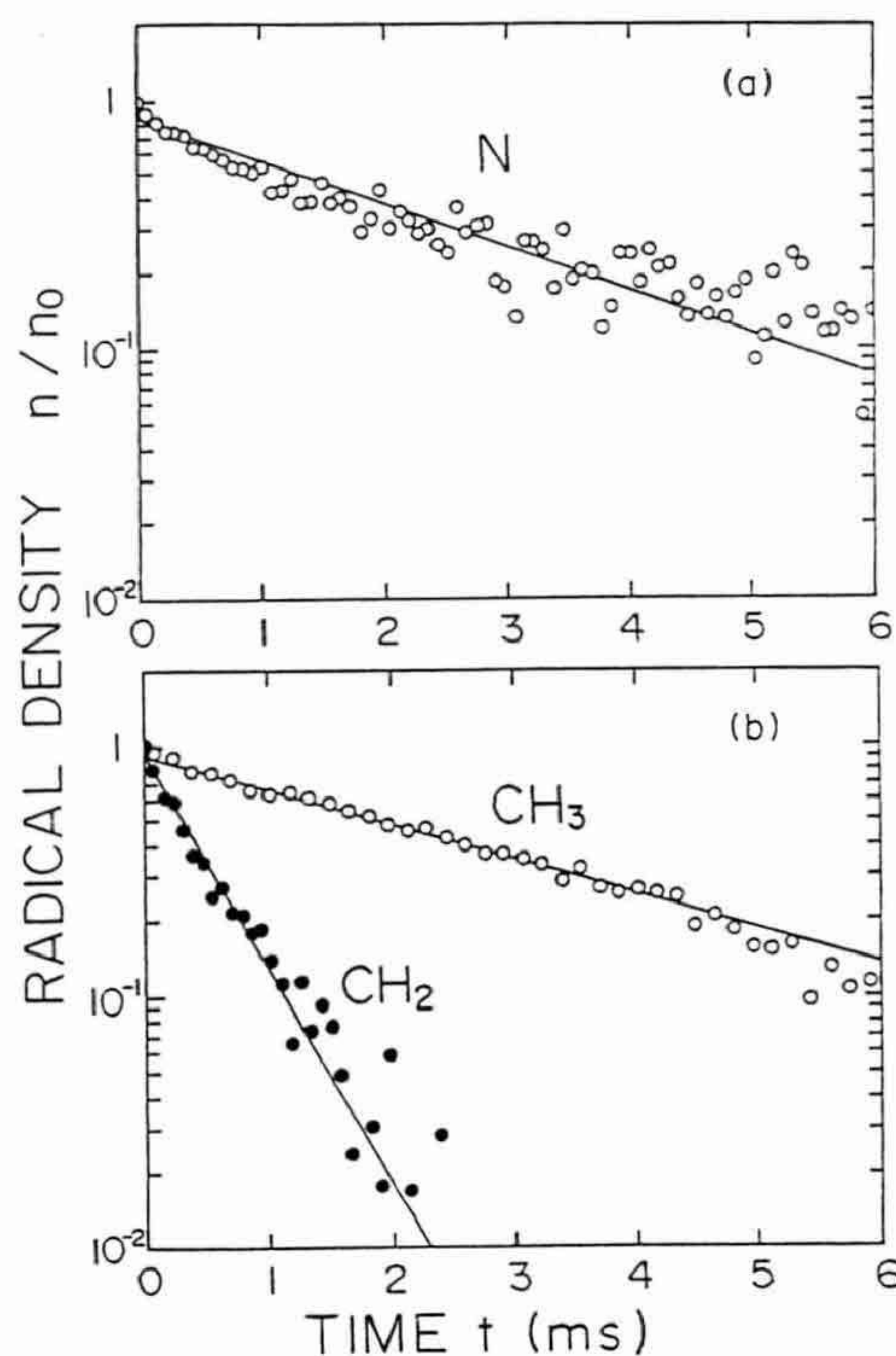
Table I. Decay time constant τ, vacuum conductance C_a and C_b, surface loss rate k, and sticking coefficient s for dissociation products N, CH_3, and CH_2.

product	τ (ms)	C_a (1/s)	C_b (1/s)	k (1/s)	s
N	2.6	0.95	0.54	4.3	0.0041
CH_3	3.1	0.99	0.56	3.2	0.0031
CH_2	0.52	0.95	0.54	27.3	0.026

$kT/\pi m)^{1/2}$ at $T = 400$ K were used. The obtained sticking coefficient of CH_2 radicals was in good agreement with the previous value ($s = 0.025$–0.028),[3,4] while the sticking coefficient of CH_3 was somewhat larger than the previous data ($s \simeq 0.001$).[2] It should be noted that the stainless steel surface of the dissociation cell was covered with a thin layer of hydrogenated amorphous carbon as a result of methane decomposition by the primary electron beam. Nitrogen atoms stuck to surfaces and recombined to yield nitrogen molecules. To our knowledge, there has been no report of the sticking coefficient of atomic nitrogen.

§4. Absolute Cross Sections and Discussion

According to eq. (4), we can assign the absolute value to the relative cross sections presented in part I of this paper, using the result of the complementary experiments described in §3. The absolute values of partial cross sections for dissociation of methane into CH_3 and CH_2 radicals are plotted in Fig. 5. When this figure is compared with Fig. 5 in part I of this paper, the cross section for CH_2 radical is enlarged about six times with its large sticking coefficient taken into account. The branching ratio of CH_3 to CH_2, i.e., the ratio of partial cross sec-

tions, is ~2 at the energy of 20–30 eV where the cross section becomes maximum. The relative cross sections reported in part I should be accurate to ~ ±20%. Contributions to the error are $S(\pm 5\%)$, $I_c(\pm 5\%)$, and $p(\pm 10\%)$ in eq. (1) of part I of this paper. On the other hand, the absolute cross sections derived here will be accurate to ±100% in the worst estimation. Contributions to the error are $\eta'/\beta(\pm 40\%)$, $\sigma'(\pm 20\%)$, $k(\pm 20\%)$, $[CH_4](\pm 10\%)$, $C_a(\pm 5\%)$, and $dS/dt(\pm 5\%)$ in eq. (4).

Melton and Rudolph[9] reported that the partial cross section at 100 eV is 1.2×10^{-20} m^2 for CH$_3$ and 0.2×10^{-20} m^2 for CH$_2$. These values are larger than the present data, and one of the reasons is that they did not adopt but assumed the ionization cross section σ' of radicals.

The solid line in Fig. 5 indicates the sum of the cross section for neutral dissociation (σ_d) and that for electronic excitation (σ_e), which was previously obtained in electron swarm studies.[10] Unfortunately, the value of σ_e cannot be discriminated from σ_d, which should be larger

than the sum of partial dissociation cross sections for CH$_3$ and CH$_2$. The sum of the present data in Fig. 5 does not exceed the value of $(\sigma_d + \sigma_e)$, and varies with the impact energy in a manner similar to the swarm results. On the other hand, Winters[1] measured the total cross section (σ_{td}) for both neutral dissociation (σ_d) and dissociative ionization (σ_{di}). The dashed line in Fig. 5 indicates the total cross section $\sigma_d(=\sigma_{td}-\sigma_{di})$, that is, Winters' data corrected by σ_{di}. Here the value of σ_{di} was calculated from the total ionization cross section[6] by subtracting the partial ionization cross section[11] for CH$_4 \rightarrow$ CH$_4^-$. It is a contradiction to the value of σ_d (Winters-corrected) being larger than the value of $(\sigma_d + \sigma_e)$ at $E > 50$ eV in Fig. 5. Moreover, the dashed line shows the rather flat dependence on the energy between 20 eV and 100 eV. The discrepancy from the present data becomes serious at higher energies since other species such as CH and C are thought to appear at the dissociation rate less than that for CH$_3$ and CH$_2$. Thus, the surface adsorption method[1] used for radical detection encounters some difficulties at high energies. For example, the surface reaction may change at high impact energies where many species of excited dissociation products react on surfaces.

Fig. 5. Experimental points of absolute partial cross sections for dissociation of methane into CH$_3$ (closed circle) and CH$_2$ (open circle). The solid line indicates the total cross section for neutral dissociation (σ_d) and electronic excitation (σ_e) after Hayashi.[10] The dashed line indicates the total cross section σ_d after being Winters corrected.[1]

References

1) H. F. Winters: J. Chem. Phys. **63** (1975) 3462.
2) H. Toyoda, H. Kojima and H. Sugai: Appl. Phys. Lett. **54** (1989) 1507.
3) H. Kojima, H. Toyoda and H. Sugai: Appl. Phys. Lett. **55** (1989) 1292.
4) H. Sugai, H. Kojima and H. Toyoda: Appl. Phys. Lett. **56** (1990) 2616.
5) P. C. Cosby: *16th Int. Conf. Physics of Electronic and Atomic Collisions, Abstract of Contributed Papers*, eds. A. Dalgarno *et al.* (1989) p. 348.
6) D. Rapp and P. Englander-Golden: J. Chem. Phys. **43** (1965) 1464.
7) H. F. Winters: J. Chem. Phys. **44** (1966) 1472.
8) E. Brook, M. F. A. Harrison and A. C. H. Smith: J. Phys. **B11** (1978) 3115.
9) C. E. Melton and P. S. Rudolph: J. Chem. Phys. **47** (1967) 1771.
10) M. Hayashi: *Swarm Studies and Electron-Molecule Collisions*, eds. L. C. Pitchford, B. V. McKoy, A. Chutjian and S. Trajmar (Springer-Verlag, New York, 1987) p. 180, and references therein.
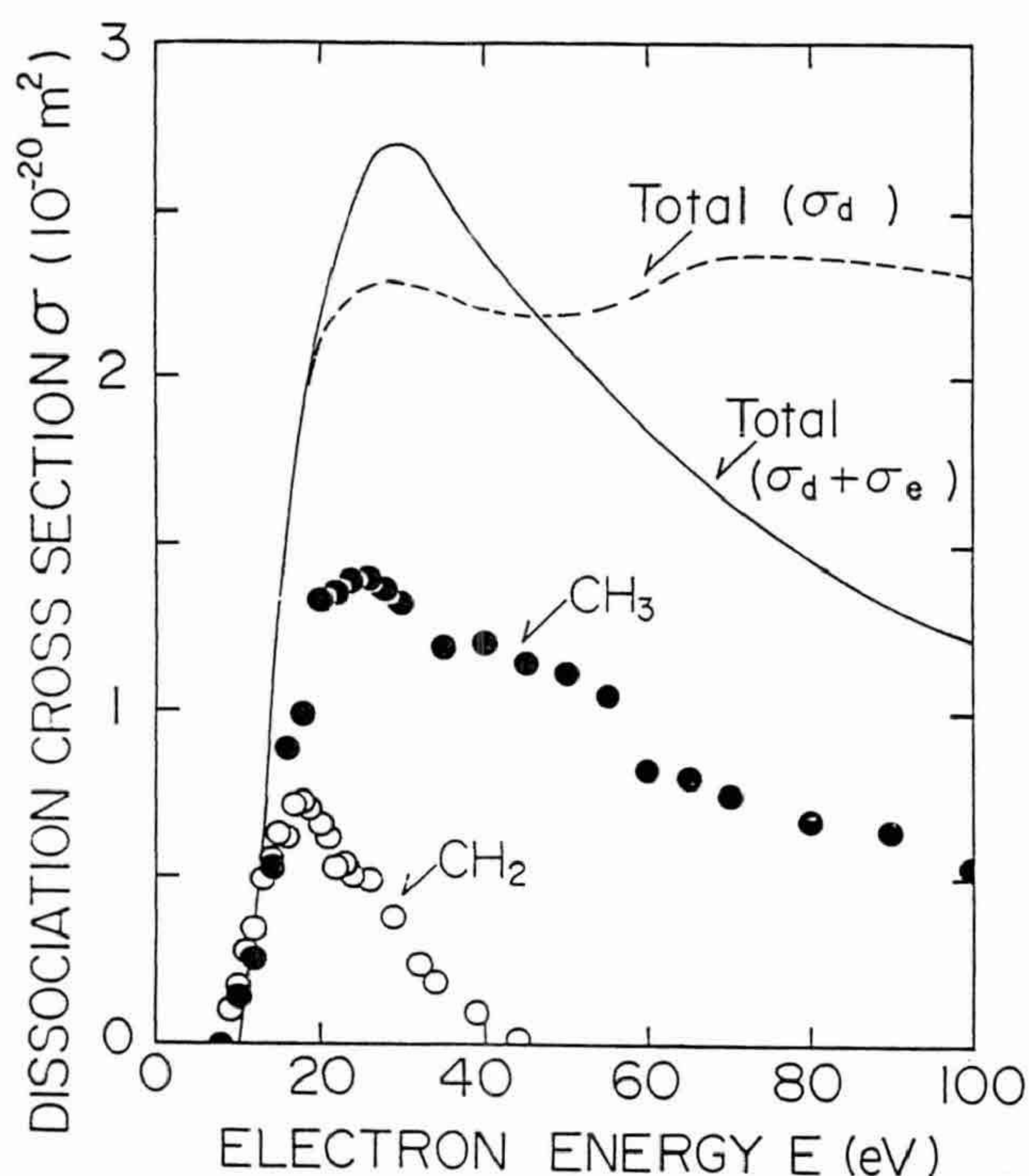11) H. Chatham, D. Hils, R. Robertson and A. Gallagher: J. Chem. Phys. **81** (1984) 1770.